Engineering atomic and molecular nanostructures at surfaces

Johannes V. Barth[1,2], Giovanni Costantini[3] & Klaus Kern[1,3]

The fabrication methods of the microelectronics industry have been refined to produce ever smaller devices, but will soon reach their fundamental limits. A promising alternative route to even smaller functional systems with nanometre dimensions is the autonomous ordering and assembly of atoms and molecules on atomically well-defined surfaces. This approach combines ease of fabrication with exquisite control over the shape, composition and mesoscale organization of the surface structures formed. Once the mechanisms controlling the self-ordering phenomena are fully understood, the self-assembly and growth processes can be steered to create a wide range of surface nanostructures from metallic, semiconducting and molecular materials.

In his classic talk of 1959, Richard P. Feynman pointed out[1] that there is "plenty of room at the bottom". He predicted exciting new phenomena that might revolutionize science and technology and affect our everyday lives — if only we were to gain precise control over matter, down to the atomic level. The decades since then have seen the invention of the scanning tunnelling microscope that allows us to image and manipulate individual molecules and atoms[2,3]. We also have access to nanostructured materials with extraordinary functional properties, such as semiconductor quantum dots and carbon nanotubes[4,5], and a growing understanding of how structural features control the function of such small systems.

These complementary developments are different aspects of nanotechnology, which aims to create and use structures, devices and systems in the size range of about 0.1–100 nm (covering the atomic, molecular and macromolecular length scales). Because of this focus on the nanometre scale, nanotechnology might meet the emerging needs of industries that have thrived on continued miniaturization and now face serious difficulties in upholding the trend, particularly in microelectronics[6] and magnetic data storage[7]. But even if nanosystems and nanodevices with suitable performance characteristics are available, nanotechnology solutions will find practical use only if they are economically viable. We will need to develop methods for the controlled mass fabrication of functional atomic or molecular assemblies and their integration into usable macroscopic systems and devices.

The two basic approaches to creating surface patterns and devices on substrates in a controlled and repeatable manner are the 'top-down' and 'bottom-up' techniques[8] (Fig. 1). The former may be seen as modern analogues of ancient methods such as lithography, writing or stamping, but capable of creating features down to the sub-100 nm range. The sophisticated tools allowing such precision are electron-beam writing, and advanced lithographic techniques that use extreme ultraviolet or even hard X-ray radiation[9]. Methods based on electron-beam writing achieve very high spatial resolution at reasonable capital costs, but operational capacity is limited by the serial nature of the process (although electron-projection methods may overcome this limitation). The next-generation production lines used by the semiconductor industry are likely to be based on X-ray lithography, which allows parallel processing. But the upgrade will require huge investments and extensive equipment development, to deal with the need for vacuum environments, short-wavelength optics, radiation sources and so on.

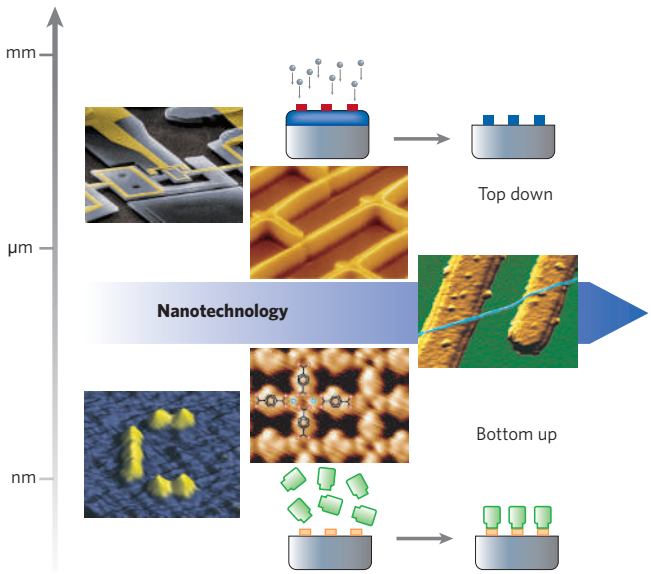

Figure 1 | Two approaches to control matter at the nanoscale. For top-down fabrication, methods such as lithography, writing or stamping are used to define the desired features. The bottom-up techniques make use of self-processes for ordering of supramolecular or solid-state architectures from the atomic to the mesosopic scale. Shown (clockwise from top) are an electron microscopy image of a nanomechanical electrometer obtained by electron-beam lithography[92], patterned films of carbon nanotubes obtained by microcontact printing and catalytic growth[93], a single carbon nanotube connecting two electrodes[94], a regular metal-organic nanoporous network integrating iron atoms and functional molecules[78], and seven carbon monoxide molecules forming the letter 'C' positioned with the tip of a scanning tunnelling microscope (image taken from http://www.physics.ubc.ca/~stm/).

[1]Institut de Physique des Nanostructures, École Polytechnique Fédérale de Lausanne, CH-1015 Lausanne, Switzerland; [2]Departments of Chemistry and Physics & Astronomy, University of British Columbia, Vancouver, British Columbia V6T 1Z4, Canada ; [3]Max-Planck-Institut für Festkörperforschung, Heisenbergstrasse 1, D-70569 Stuttgart, Germany.

Considerable efforts have also been invested in developing and exploring alternative top-down patterning methods. A particularly versatile, rapid and low-cost technique is microcontact printing[10], which uses soft and hard stamps to transfer patterns with feature sizes above 100 nm onto a wide range of substrates; however, it becomes increasingly demanding for smaller feature sizes. Ultimate precision is achieved with scanning probe techniques, which are now an established (albeit cumbersome) method for the direct writing and positioning of individual atoms[3]. Prototype scanning force arrays that operate massively in parallel and thus multiply throughput have recently been developed[11], but scanning probe methods seem unlikely to find industrial use in the near future.

Top-down methods essentially 'impose' a structure or pattern on the substrate being processed. In contrast, bottom-up methods aim to guide the assembly of atomic and molecular constituents into organized surface structures through processes inherent in the manipulated system. Here, we outline how self-organized growth and self-assembly at well-defined surfaces (some of which may have been created using top-down methods) can serve as an efficient tool for the bottom-up fabrication of functional structures and patterns on the nanometre scale. We focus on atomic-level investigations and highlight what we regard as particularly informative illustrations of how this approach might lead to useful nanometre-scale surface structures. A brief introduction to the elementary processes governing surface self-ordering provides a foundation for the subsequent discussion of how these processes can be tuned in metallic, semiconducting and molecular systems to obtain surface structures with desired geometric order and well-defined shapes.

Basic concepts in surface structuring

Common to all bottom-up strategies for the fabrication of nanostructures at surfaces is that they are essentially based on growth phenomena. Atoms or molecules (or both) are deposited on the substrate (in vacuum, ambient atmosphere or solution) and nanometre-scale structures evolve as a result of a multitude of atomistic processes. This is inherently a non-equilibrium phenomenon and any growth scenario is governed by the competition between kinetics and thermodynamics. We thus use the term 'self-organized growth' to describe autonomous order phenomena mediated by mesoscale force fields or kinetic limitations in growth processes, whereas 'self-assembly' is reserved for the spontaneous association of a supramolecular architecture from its molecular constituents[12–14]. The term 'self-organization', in contrast to self-organized growth and self-assembly, is usually used in a different context, as it relates to dissipative structure formation in systems far from thermodynamic equilibrium[15] and the initial emergence of biological macromolecules[16].

The primary mechanism in the growth of surface nanostructures from adsorbed species is the transport of these species on a flat terrace (see Fig. 2), involving random hopping processes at the substrate atomic lattice[17,18]. This surface diffusion is thermally activated; that is, diffusion barriers need to be surmounted when moving from one stable (or metastable) adsorption configuration to another. As is typical for such processes, the diffusivity D — the mean square distance travelled by an adsorbate per unit time — obeys an Arrhenius law; this holds for atoms as well as rigid organic molecules[19]. If we now consider a growth experiment where atoms or molecules are deposited on a surface at a constant deposition rate F, then the ratio D/F determines the average distance that an adsorbed species has to travel to meet another adsorbate, either for nucleation of a new aggregate or attachment to an already formed island. The ratio of deposition to diffusion rate D/F is thus the key parameter characterizing growth kinetics. If deposition is slower than diffusion (large values of D/F), growth occurs close to equilibrium conditions; that is, the adsorbed species have enough time to explore the potential energy surface so that the system reaches a minimum energy configuration. If deposition is fast relative to diffusion (small D/F), then the pattern of growth is essentially determined by kinetics; individual processes, notably those leading to metastable structures, are increasingly important.

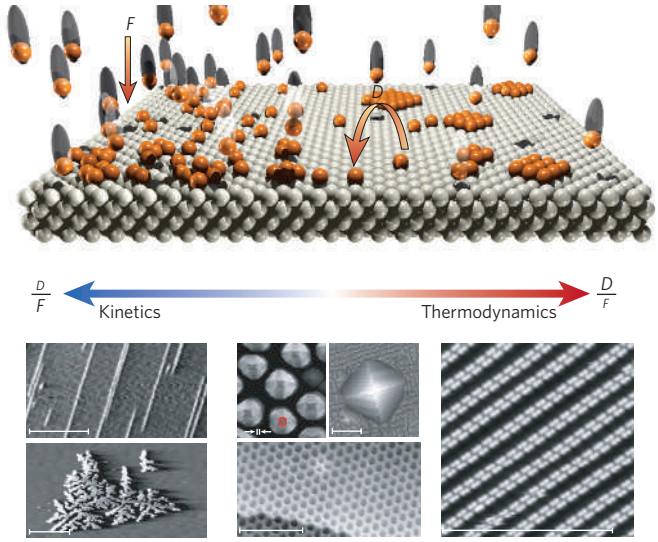

Figure 2 | Atomic-scale view of growth processes at surfaces. Atoms or molecules are deposited from the vapour phase. On adsorption they diffuse on terraces to meet other adspecies, resulting in nucleation of aggregates or attachment to already existing islands. The type of growth is largely determined by the ratio between diffusion rate D and deposition flux F. Metallic islands are controlled by growth kinetics at small D/F values. The hierarchy in the barrier of diffusing atoms can be translated into geometric order and well-defined shapes and length scales of the resulting nanostructures. The micrographs on the left-hand side show monatomic Cu chains grown on an anisotropic Pd(110) substrate (upper image) and Ag dendrites on hexagonal Pt(111) (ref. 20) (lower image). Semiconductor nanostructures are usually grown at intermediate D/F and their morphology is determined by the complex interplay between kinetics and thermodynamics. Strain effects are particularly important and can be used to achieve mesoscopic ordering. The micrographs in the centre show pyramidal and dome-shaped Ge semiconductor quantum dots grown on Si(100)[95] (upper right and upper left panels, respectively) and a boron nitride nanomesh on Rh(111)[96] (lower panel). To allow for supramolecular self-assembly based on molecular recognition, conditions close to equilibrium are required (large D/F values, or post-deposition equilibration). The micrograph on the right shows as an example a supramolecular nanograting of rod-like benzoic acid molecules on Ag(111). It consists of repulsively interacting molecular twin chains, which are stabilized by intermolecular hydrogen bonds[26]. Scale bars, 20 nm in every image.

Low-temperature growth of metal nanostructures on metal surfaces is the prototype of kinetically controlled growth methods. Metal bonds have essentially no directionality that can be used to direct interatomic interactions. Instead, kinetic control provides an elegant way to manipulate the structure and morphology of metallic nanostructures. On homogeneous surfaces, their shape and size are largely determined by the competition between the different movements the atoms can make along the surface, such as diffusion of adatoms on surface terraces, over steps, along edges and across corners or kinks. Each of these displacement modes has a characteristic energy barrier, which will to a first approximation scale with the local coordination of the diffusing atom: the diffusion of an atom over a terrace will have a lower energy barrier than diffusion along an edge or crossing of a corner, and descending an edge is often an energetically more costly process than terrace diffusion. A given material system thus has a natural hierarchy of diffusion barriers associated with these different atomistic processes. This makes it possible to shape growing aggregates by selective activation or suppression of particular diffusion processes through external growth parameters (temperature and metal deposition flux) and through the choice of a substrate with appropriate symmetry[20]. Judicious tuning of the relative importance of different diffusion processes has allowed on-demand fabrication of a host of metal nanostructures, ranging from small compact uniform clusters and large

faceted islands to fractals, dendrites and atomically thin chains[17,18,20–22].

For metals, then, formation of surface structures can be controlled only by controlling the complex kinetics of the different diffusion processes at play, given the high energies associated with covalent bond formation and the limited information for spatial organization. In contrast, molecules that can participate in weak and directional non-covalent bonds may be programmed to form desired supramolecular structures[23]. The basic concepts ruling the self-assembly of three-dimensional supramolecular structures can also guide the assembly of adsorbed molecules into low-dimensional supramolecular systems that show a high degree of order on the nanometre scale. The approach does not require control over a hierarchy of activated diffusive motions, but operates near equilibrium conditions where the D/F ratio is a circumstantial parameter. Ordering may occur after deposition, and in favourable situations self-correction through the elimination of transiently formed defective structures is possible. The parameters crucial for this type of structure control are the surface mobility of molecules, their lateral interactions and their coupling to the surface atomic lattice. These depend on the chemical nature of the system and the atomic environment and symmetry of the substrate[19,24,25], all of which can be used to tune the delicate balance of lateral interactions and molecule–substrate coupling in order to steer supramolecular organization towards the desired structures[26].

If surface-supported nanostructures are to be organized on the mesoscale (10–1,000 nm), then at least some of the forces used for that purpose need to act over length scales comparable to the desired feature size; that is, they must be much longer-ranging than atomic distances. Such long-range forces can arise from various physical effects, including elastic and electrostatic interactions. Elastic forces are generally relevant to surfaces and epitaxial systems, given that atoms on a surface or in an epilayer are always under stress, even in the case of pristine surfaces or homoepitaxial systems[27]. The resultant forces typically give rise to regular two-dimensional strain relief or reconstruction patterns[21,22,28,29] with feature sizes of 2–20 nm, which can then serve as templates to control the growth of further patterns. In heteroepitaxial systems, the elastic energy associated with the inherent lattice mismatch of the materials can induce not only such lateral ordering, but also three-dimensional aggregation. 'Stranski–Krastanow growth', in which three-dimensional islands form spontaneously above a critical film thickness, is a well-established method for creating semiconductor quantum dots[30]. This nanostructure formation process is driven by thermodynamics (that is, strain relief overcompensates for the increase in surface energy associated with the transition to three-dimensional growth), but the resulting structures are usually metastable and their exact shape, size and composition result from a delicate interplay between thermodynamic and kinetic effects.

Magnetism at the physical limit

Gordon Moore observed in 1965 that improved fabrication technologies resulted in the doubling of the number of silicon field-effect transistors per unit area roughly every 18 months. 'Moore's law', which has achieved almost cult status, still describes with remarkable precision the advances in complementary metal oxide semiconductor (CMOS) technology that continue to increase information processing speeds. But the exponential growth of the information industry relies just as much on improvements in data storage, which uses small regions of ferromagnetic material with opposite magnetization to store 'zeros' and 'ones' in a hard disk. The continued downscaling of these storage domains outperforms even the stunning development of CMOS technology. During the past decade, storage density has doubled almost every 12 months and has reached 100 Gbit per square inch today. But as in the case of CMOS technologies, the drive for further miniaturization faces fundamental physical limits[6,7]. The decrease in ferromagnetic domain size is accompanied by a decrease in the magnetic anisotropy energy K, which prevents spontaneous changes in magnetization direction. For very small domains, K is comparable to thermal energies so that thermal fluctuations can randomly flip the magnetization direction. This renders the domains superparamagnetic, with all stable magnetic order lost. The effect can be quantified by considering that for a single domain, the time for reversal of the magnetization orientation due to thermal fluctuations follows an Arrhenius law of the type $\tau = \tau_0 \exp(nK/k_B T)$ (here τ_0 is a pre-factor of the order of 10^{-9} s, n the number of atoms in the domain, k_B the Boltzmann constant). For magnetic anisotropy energies of 40 μeV per atom (a characteristic value for bulk hexagonally close-packed cobalt) and a typical stability requirement of $\tau > 10$ years, magnetically stable nanostructures thus need to contain roughly $n \approx 10^5$ atoms. In today's recording media, several hundred to a thousand of such individual domains are needed to realize one magnetic bit that can be reliably written and read, with high signal-to-noise ratio. Clearly, if miniaturization is to result in further increased storage capacities, we need to extend or avoid the superparamagnetic limit.

An obvious strategy is to develop new materials and structures with a substantially higher anisotropy energy K. A useful pointer is that K depends on spin–orbit interactions and on orbital magnetic moments, and hence on the precise atomic structure of magnetic materials[31,32]. The orbital magnetic moment m_L is particularly sensitive to the local atomic configuration and influences the magnetocrystalline anisotropy. In bulk materials m_L is largely quenched through the crystal field; but in low-dimensional nanostructured materials, the reduced symmetry of the electron wavefunctions can result in strongly anisotropic orbital magnetization that will boost the magnetocrystalline contribution to the anisotropy energy. This effect should be particularly pronounced for atomic-scale structures with constituent atoms that have a reduced average coordination, which in turn results in m_L values approaching those typically seen for free atoms[33]. The effect will be significant for structures that range in size from the single adatom to clusters composed of a few atoms to several tens of atoms at most, and it is difficult to envisage their efficient production without the use of bottom-up fabrication methods[34,35].

Judiciously used, self-organized metal growth on surfaces can produce a variety of useful nanoscale patterns with high densities in a fast, parallel process[20]. For example, the step decoration method[36,37] allows ready formation of uniform arrays of cobalt chains on a Pt(997) surface. The method makes use of the fact that step edges act as preferential nucleation sites for the deposited cobalt atoms, because of the increased coordination experienced at step sites relative to terrace sites. Growth in a well-defined temperature range then results in uniform cobalt chains of monatomic width over the entire sample, forming dense arrays of parallel one-dimensional nanowires. By adjusting the cobalt coverage on the surface and the average step spacing of the platinum surface, width and separation of the nanowires can be independently controlled. Similarly, bimetallic islands containing a Pt core and Co rim are readily obtained by Pt deposition and annealing to create the core islands, followed by Co deposition and annealing to create the rim[38].

Such surface-supported cobalt nanostructures, when examined, reveal how magnetic properties change as the size of the structures is reduced to a few atoms[39,40]. In the case of two-dimensional cobalt clusters on Pt(111), orbital moment and magnetic anisotropy energy increase markedly as the cluster size decreases (Fig. 3a). The orbital moment increases from $m_L = 0.3\ \mu_B$ (where μ_B is the Bohr magneton) for clusters composed of about 10–15 atoms, to 0.59 μ_B for tetramers and 0.78 μ_B for trimers, and to a maximum value of 1.1 μ_B for a single adatom. The latter's orbital moment is more than seven times the bulk value. The magnetic anisotropy energy K shows a similar trend (Fig. 3a), reaching values as large as 9.3 meV for a single adatom[40]. Atomic-scale Co nanostructures may thus have K values up to two orders of magnitude larger than that of bulk hexagonal close-packed (h.c.p.) cobalt. Typical magnetic recording materials such as Co/Pt multilayers and even the permanent magnet $SmCo_5$ also have significantly lower K values ($K \approx 0.3$ meV atom^{-1} and $K \approx 1.8$ meV atom^{-1}, respectively) than the cobalt nanostructures. This pronounced size depen-

dence of magnetic properties arises from the low coordination of Co atoms in the atomic-scale nanostructures, which can reduce *d*-state hybridization and the crystal field potential that is produced by the electric field of neighbouring lattice atoms. We expect that detailed insight into the effects of coordination number on both m_L and K will open new avenues for the design of nanostructures with promising magnetic properties. For example, the magnetic anisotropy of two-dimensional (2D) bimetallic islands with Pt core and Co rim is entirely determined by the rim of Co atoms at the perimeter, which accounts for extreme anisotropy energies[38].

Two-dimensional Co nanoparticles are superparamagnetic down to the lowest temperatures. In contrast, monatomic Co chains containing on average 80 atoms (Fig. 3b, c) are ferromagnetic[39] at 4.2 K. The observation of a paramagnetic response at 45 K implies the absence of single-domain 1D ferromagnetic coupling, but the shape of the magnetization curve reveals the onset of short-range magnetic order, with spins coupling into local blocks of roughly 15 atoms. Long-range order is forbidden in infinite 1D systems at true equilibrium, yet it may exist in finite systems over relatively short timescales. In the case of the monatomic Co chain, a transition into a long-range ferromagnetically ordered state occurs at 15 K and is evident from the hysteresis in the magnetization curve (see Fig. 3c). This behaviour is due to the low coordination of the Co atoms on the vicinal Pt substrate, which results in a large anisotropy energy of 2.1 meV atom^{-1} that locks the magnetization of each spin block along the easy axis of the system. On the timescale of the experiment, ferromagnetic coupling thus effectively extends over the entire chain array[41] and gives rise to the smallest elemental magnet yet fabricated.

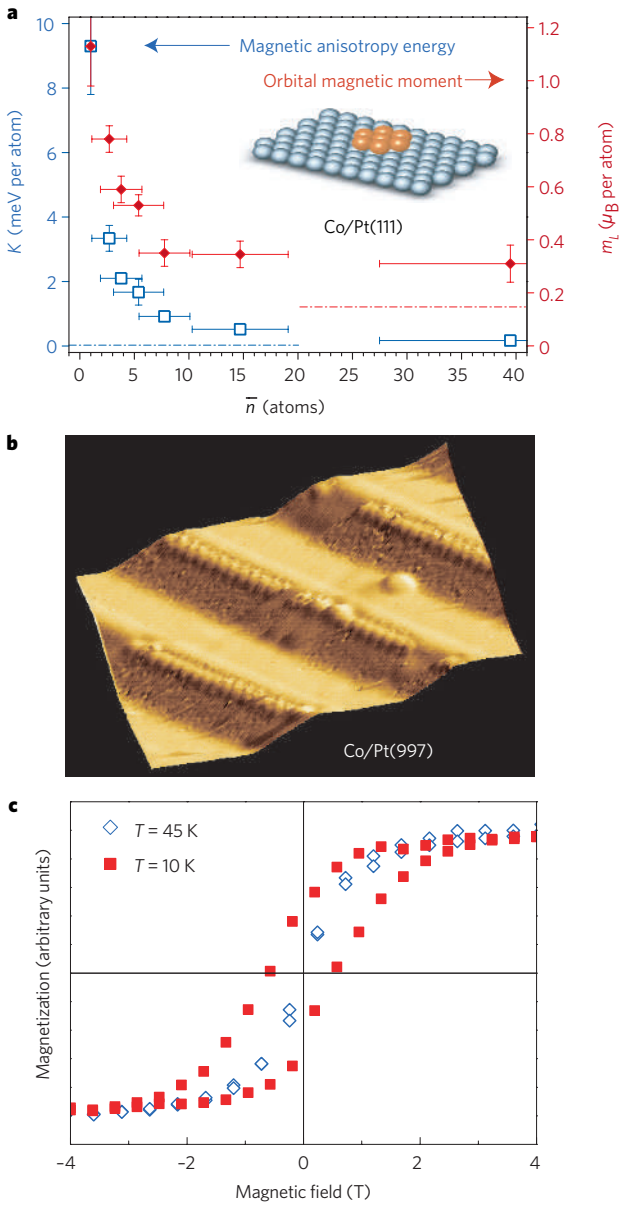

Figure 3 | Magnetism at the spatial limit. a, Magnetic anisotropy energy K (squares) and orbital magnetic moment m_L (diamonds) of Co atoms and two-dimensional clusters at the Pt(111) surface as a function of size n. The dashed lines represent the K and m_L values for bulk h.c.p. Co (blue and red, respectively)[40]. **b**, Scanning tunnelling microscopy image of monatomic cobalt chains decorating the steps of a regularly stepped platinum surface. The average distance between neighbouring chains is 2 nm. **c**, On cooling below 15 K, Co blocks become ferromagnetic, indicated by the opening up of a hysteresis loop in the magnetization curve[39].

The magnetic behaviour seen in Co nanostructures is not only relevant for our fundamental understanding of low-dimensional magnetism, but has important implications for magnetic data storage technology. That is, the increase in magnetic anisotropy energies by more than two orders of magnitude, relative to the values seen in more traditional transition-metal systems, implies that a few hundred cobalt atoms might suffice to realize a stable magnetic bit at room temperature.

Semiconductor artificial atoms

In metallic nanostructures, because of the effects of coordination, every atom 'counts' with respect to the magnetic properties. For semiconductor materials, functional properties tend to be less sensitive to the exact number of constituent atoms: desired quantum effects already arise for structures with dimensions of 10–100 nm and containing somewhere between 10^3 and 10^6 atoms in a crystalline lattice. In this size range, the energy spectrum of electrons and holes confined in all three dimensions within these 'quantum dots' becomes discrete and in many ways similar to the spectrum of atoms[4]. Still, quantum dots are very much solid-state nanostructures, and their energy spectrum, which controls many of the physical properties of interest, can be adjusted over a wide range by tuning composition, size, lattice strain and morphology. These features make semiconductor quantum dots attractive for the design and fabrication of new electronic, magnetic and photonic devices and other functional materials.

Semiconductor quantum dots are often prepared as colloidal nanocrystals (see the review in this issue by Yin & Alivisatos, p. 664) but here we will focus only on semiconductor quantum dots supported on surfaces or embedded in solids. These systems can be prepared by using a wide range of methods, including lithography, etching and site-selective implantation[42]. But fabrication methods based on self-organized growth at surfaces are particularly attractive because they yield quantum dots with virtually no interface defects that might adversely affect performance, and because they can produce particularly small structures with widely separated energy levels that are essential for room-temperature operation. The approach can also produce high-density quantum dot structures in a fast, parallel process that is compatible with existing semiconductor technology and therefore permits mass fabrication and high levels of integration. However, to use self-organized growth effectively for quantum dot fabrication, we need detailed insight into the nucleation and growth processes involved, so as to tune the dot properties precisely and control their intrinsic statistical inhomogeneity.

As so many physical properties depend on quantum dot size and shape, it is essential to know the actual morphology of the 3D semiconductor islands that form on deposition of atoms from the gas phase, and to know how they evolve during post-growth treatments. But even though these systems have been intensely studied for more than a decade and many of their electronic and optical properties characterized, the structure of nucleated semiconductor islands and their subsequent morphological evolution remain incompletely understood. It is therefore encouraging that a common framework[43] can describe quantum dots that develop in the two most studied model

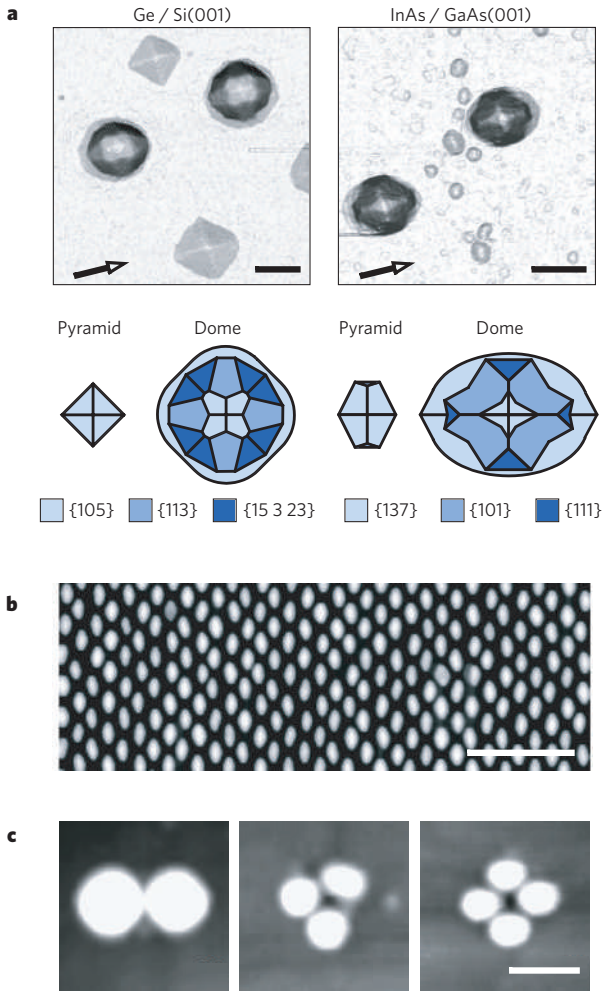

Figure 4 | Semiconductor quantum structures. **a**, Scanning tunnelling microscope images of pyramid and dome islands for the two main representative systems in semiconductor lattice-mismatched heteroepitaxy. The corresponding schematic structural models are also shown[43]. **b**, Atomic force topography of a regular array of InGaAs quantum dots reflecting self-organized growth on a prestructured GaAs(001) substrate[50]. **c**, Lateral quantum dot molecules grown in the InAs/GaAs(001) system. Bi-, tri- and quad-molecules can be produced by adjusting the substrate temperature and amount of deposited material[60]. Scale bars correspond to 50 nm in **a** and **c**, and to 500 nm in **b**.

systems: during the growth of Ge on Si(001) and during the growth of InAs on GaAs(001). The two types of quantum dots are both produced in the Stranski–Krastanow growth mode, with defect-free but strained 3D islands forming spontaneously on top of a thin wetting layer during lattice-mismatched heteroepitaxial growth. In both systems, only two discrete, well-defined families of islands develop: small islands that are bounded by one type of shallow facets and referred to as pyramids, and larger, multi-faceted islands that are characterized by steeper facets and referred to as domes (see Fig. 4a). When overgrowing the initially formed islands with the substrate material (Si and GaAs, respectively) to create the actual quantum dots, the capping process in both systems involves extension of the shallow facets at the expense of the steeper ones and a considerable reduction in island height. These experimental observations confirm theoretical predictions[44] that common, well-defined island shapes occur during growth and evolution, independent of the specific material system considered. It might therefore be possible to develop a common framework to explain at least qualitatively island growth and evolution for many material combinations that follow the Stranski–Krastanow growth mode. We expect the availability of such a universally applicable descriptive model to have considerable impact on our ability to design and engineer quantum dot structures.

In addition to controlling the properties of individual quantum dots, many of the applications so far envisaged also require precise arrangement of these structures into ordered arrays. For example, regular arrangement is obvious for systems or devices that require the addressing or coupling of individual quantum dots or the further processing of quantum dot signals, as in the case of single-electron[45], single-photon[46] and quantum computation[47] devices. Similarly, uniformity in position and spacing is critical for applications that make use of quantum dot ensembles, and where overall device performance depends on the mutual interaction between the individual dots (as in the case of cellular automata based on quantum dots[48], discussed below). But a high degree of lateral order has the additional advantage that formation of these structures usually ensures high uniformity in quantum dot properties, as statistical fluctuations are greatly suppressed if each dot experiences the same local environment during growth.

Quantum dots may be laterally organized using self-ordering processes that are mediated by elastic interactions, or using patterned substrates to direct their growth. The former approach depends on the same forces that induce the spontaneous formation of islands in the Stranski–Krastanow growth mode, and will drive the ordering of islands on length scales of the same order of magnitude as the size of the islands[49]. But it is almost impossible to obtain defect-free mesoscopic quantum dot arrangements based on this approach only. In contrast, highly regular structures are readily obtained by using electron-beam or optical lithography (top-down methods) first to create patterned substrates, which then serve as templates to direct the self-organized Stranski–Krastanow growth of three-dimensional semiconductor islands (a bottom-up method). The artificial periodic modulations of the surface are thus translated into perfect quantum dot arrays[50,51], as illustrated by the example shown in Fig. 4b. A further advantage of this approach is that it allows the resulting quantum dot structures to be connected to larger structures for integration into complex devices.

Efforts to controllably fabricate and characterize semiconductor quantum dots have mainly been driven by the desire to develop systems that take advantage of their extremely small dimensions and low power dissipation. For example, the performance of lasers can be substantially improved by using quantum dots as the active medium[52]. The tunable and discrete energy levels typical of quantum dots mean that the choice of emitted wavelength can be adjusted with unprecedented flexibility; the small active volume permits laser operation at low power, high frequency and low threshold currents that are independent of the working temperature. Information technology is another field in which the properties of quantum dots might prove attractive. One example is a cellular automaton[48] in which binary information is encoded in the configuration of charge distributed among the quantum dots and interaction between the dots provided by Coulomb interactions. Such an ensemble, with appropriately designed dot arrangement, is an essentially classical device that can reproduce the effect of wires and logic gates and implement any complex Boolean operation[53]. But quantum dots are also attracting interest for quantum computation applications, where information is encoded using quantum two-state systems ('qubits') that can be prepared in a superposition of the two states and thus enable dramatic increases in computing capabilities[54–56]. The basic building block is a two-qubit quantum gate that performs unitary operations on one qubit depending on the (quantum) state of the other[57]. Such a gate can be realized using quantum dot molecules; that is, sets of quantum-mechanically coupled quantum dots whose charge carrier wavefunctions are delocalized over the entire structure. The first semiconductor quantum dot molecules with controlled separation between the dots have been fabricated using top-down methods[58], although their sensitivity to thermal perturbations precludes any scope for use in 'real world' devices. Decreasing the size of the quantum dots should allow

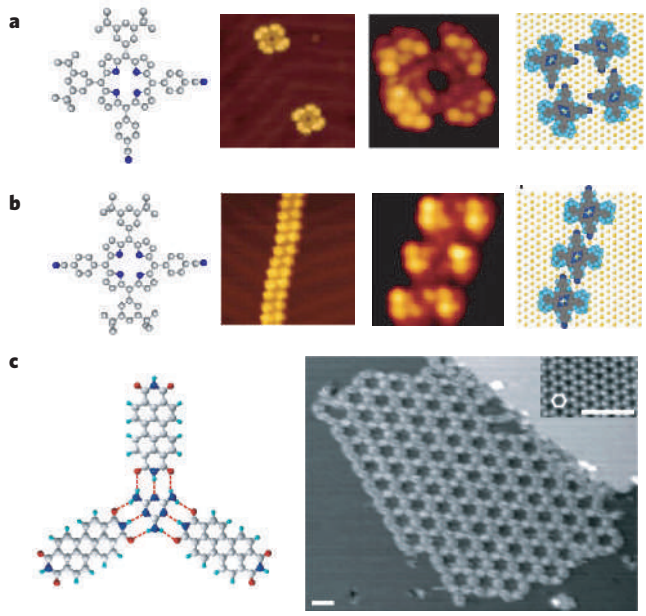

Figure 5 | Steering self-assembly of supramolecular nanostructures using hydrogen-bonding. **a**, **b**, Porphyrins substituted with two functional cyanophenyl moieties in a *cis* or *trans* configuration[67]. **a**, The *cis* species assembles in compact clusters of four molecules. **b**, With the *trans* species linear molecular chains are obtained. Mesoscopic ordering is in both cases dictated by the preferential attachment at the elbows of the chevron reconstruction of the Au(111) substrate used, visible as weak corrugation lines. Imaged area at left (right) is 20 nm^2 (5.3 nm^2). **c**, The complementary tectons perylene tetracarboxylic di-imide and melamine form a trigonal motif, where each intermolecular linkage is stabilized by three hydrogen bonds. This repeat unit gives rise to the regular nanoporous honeycomb layers fabricated on the hexagonal Ag-passivated Si(111) substrate shown in the inset[75]. Scale bars, 3 nm.

room-temperature operation. But controlled formation and precise arrangement of such small structures are challenging and likely to require self-organized growth, as illustrated by a strategy that makes use of spontaneous alignment of stacked quantum dot layers to form vertical quantum dot molecules[59]. The selective addressing of specific quantum gate parts is likely to be more feasible using laterally coupled quantum dot molecules, which have now also been produced through self-organized growth[60,61]. Figure 4c shows quantum dot molecules containing two, three and four dots; these were created in InAs/GaAs(001) using an elaborate growth–overgrowth–etching–regrowth procedure that is primarily based on self-organized growth[60]. The electronic properties of these quantum dot molecules remain to be explored, but their structural characteristics and the ability to combine them into highly ordered arrays are promising.

Supramolecular engineering

The range of functional nanometre-sized structures that can be fashioned from metallic or semiconducting materials through self-organized growth is inevitably somewhat limited, in that design and fabrication methods need to be based on the functional and structural features inherent in these materials. This contrasts with the construction of molecular nanoscale structures and patterns: the power of chemical synthesis provides access to a potentially vast range of functionally and structurally diverse building blocks ('tectons'), which can be linked through different types of relatively weak, non-covalent interactions (predominantly hydrogen bonds and metal–ligand interactions) to yield organized supramolecular architectures with tailor-made properties[14,23,62]. But although much is known about how supramolecular chemistry — the chemistry of the intermolecular non-covalent bond — can be tuned to create desired supramolecular crystals or supramolecular compounds in solution, this knowledge cannot be directly translated to guide the assembly of adsorbed molecules into larger surface structures[63,64]. To do so, the influence of the substrate atomic lattice and substrate electronic structure on non-covalent bonds needs to be fully understood. For example, the substrate used will often alter the electronic properties of adsorbed ligands so that solution-based coordination chemistry concepts cannot be applied without appropriate modification[65]. Interactions between adsorbed molecules and their substrate may also perturb the surface-state free electron gas in metallic substrates, which in turn can influence how adsorbates are arranged on the surface[66]. More direct effects are that substrates may be reactive and chemically modify the functional moieties of the adsorbed building blocks, and the fact that topological surface features can influence interactions between adsorbed species for geometric reasons. These various effects make it obviously difficult to translate supramolecular concepts developed for crystals or solutions; but they can be used as tools for steering non-covalent interactions through the choice of templates with appropriate symmetry, surface patterns or chemical functions.

Planar molecules with extended π-systems have found particularly wide use because they tend to bond to surfaces in a flat-lying geometry, which allows functional groups at the molecular periphery to approach each other easily and to engage in non-covalent interactions. Provided the molecules retain mobility on the substrate with their functional groups not obstructed by the surface, supramolecular surface structures readily form as a result of two-dimensional self-assembly: the lateral coupling of suitably designed tectons. The tunability of supramolecular surface patterns through tecton design is illustrated in Fig. 5a, b[67]: the exact position of two cyanophenyl substituents at the periphery of a porphyrin core steers the intermolecular hydrogen bonding that provides lateral coupling and hence dictates the structure of the assemblies formed on a gold surface. Whereas the *cis* configuration gives rise to discrete clusters made up of four molecules (Fig. 5a), the *trans* configuration produces extended one-dimensional supramolecular chains (Fig. 5b). The spatial distribution of these clusters and chains is dictated by the surface pattern of the gold surface, which in the case of the Au(111) surface used results from a chevron reconstruction[28]. A similar influence on supramolecular ordering is seen in the case of 1-nitronaphthalene[68], emphasizing that patterned substrates are generally useful to guide the formation of low-dimensional molecular nanostructures[69,70].

A systematic study of the self-assembly behaviour of 4-[trans-2-(pyrid-4-yl-vinyl)]benzoic acid (PVBA) illustrates how the materials characteristics and symmetry of the substrate can affect the subtle balance between intermolecular interactions and molecule–surface interactions. The rod-like PVBA molecule, which contains a benzoic acid head group and a pyridyl tail group, self-assembles through head-to-tail hydrogen bonding[26,71]. If metallic palladium is used as substrate, molecule–substrate coupling is strong and dominates over intermolecular interactions; this prevents the formation of regular surface patterns. On close-packed noble-metal surfaces, the PVBA molecules are more mobile and able to assemble into highly regular, one-dimensional supramolecular arrangements resembling 'nanogratings' (see for example the scanning tunnelling microscope image reproduced in Fig. 2)[26]. Each stripe in the nanograting consists of two discrete chains of hydrogen-bonded PVBA molecules. The chains making up one stripe are held together through weak interchain hydrogen bonds, and the patterning of the stripes relative to each other appears to be due to interchain repulsions. The stripes are each about 1 nm wide, but the periodicity of the grating can be tuned from about 2 to 10 nm by controlling how much PVBA is deposited, or by taking advantage of the fact that they preferentially assemble at dislocation arrays of reconstructed substrates such as Au(111)[71,72]. Surface feature control at the molecular length scale is beyond the limits of current lithographic techniques. But for the self-assembled patterns to find practical use, methods need to be developed to transform the molecular arrangements into more rigid structures while retaining their precise spatial organization.

Extended 2D open network structures have been created using a number of different systems. One example is trimesic acid (TMA, $C_6H_3(COOH)_3$), in which regular dimerization of the carboxyl groups present results in an open network structure that reflects the molecule's three-fold symmetry[73,74]. This pattern is also encountered in organic TMA crystals, illustrating that in favourable cases motifs from organic solids can be replicated on surfaces. Another extended network structure is based on the classic H-bond motif of the melamine–cyanuric acid system, with perylene tetracarboxylic diimide serving as linear linker and melamine as trigonal connector. As illustrated in Fig. 5c, self-assembly through triple H-bond coupling yields a 2D bimolecular honeycomb network[75]. The high degree of order obtained on a substrate with appreciable surface corrugation (Ag-passivated Si(111)) emphasizes that even though individual intermolecular couplings may be weak, multiple weak linkages nevertheless enable stable and regular assemblies to form. Network stability is an essential feature if nanoporous surface patterns are used as templates to guide the formation of subsequent layers, as demonstrated by the formation of regular C_{60} arrays on the 2D bimolecular honeycomb arrangement[75].

Metal–ligand interactions are generally stronger than hydrogen bonds and thus result in more robust entities. Moreover, the incorporation of metal centres increases the scope of the functional properties of the nanoarchitectures and allows us to use design strategies based on metal-directed assembly[76,77]. This makes the controlled fabrication of surface structures based on metal–organic coordination appealing, but the approach can be challenging. Difficulties arise from the tendency of deposited metal atoms to interact strongly with the substrates used, in extreme cases resulting in surface reconstruction or alloying. Consequently the deposition sequence and substrate temperature have to be carefully controlled to avoid spurious effects and to achieve the formation of regular nanosystems.

We illustrate the principles underlying the interaction of organic linker molecules and transition metals at surfaces with the coordination behaviour of benzenepolycarboxylic acid species and iron (Fe) atoms on a copper Cu(100) surface. This system forms a variety of two-dimensional surface-supported open networks. The basic architectural motif of these networks depends on the relative concentrations of metal atoms and ligand molecules, with careful tuning of this ratio resulting in mononuclear metal-carboxylate clusters, 1D coordination polymers or fully connected 2D networks. The mononuclear complexes (Fig. 6a) are obtained[78] on depositing about 0.3 Fe atoms per linear terephthalate linker molecule (TPA, $C_6H_4(COO)_2$). As indicated in the scheme, a central Fe atom is coordinated to four TPA molecules through Fe-carboxylate bonds, with the resultant $Fe(TPA)_4$ complexes organized in a (6×6) unit cell with respect to the substrate. The complexes form a highly ordered array that covers entire terraces of the substrate, with this perfect long-range organization suggested[78,79] to result from weak hydrogen-bonding interactions between the complexes. The individual Fe centres are thus arranged in a perfect square lattice with a 15 Å periodicity. Clearly, any attempt to position large-scale arrays of single Fe atoms in a similar way using a top-down technique would be prohibitively time-consuming, if not impossible.

Increasing the amount of deposited metal to about 1 Fe atom per linker molecules results in networks of polymeric ladder structures, as illustrated in Fig. 6b for the system based on trimellate as linker[80]. This network frequently covers entire substrate terraces and constitutes a regular array of open nanocavities, each with an effective opening of (3×10) Å^2. Increasing the metal concentration further, to about two Fe atoms per linker molecule, yields fully interconnected 2D metal–organic networks with complete two-dimensional reticulation[78,80]. Examples are shown in one of the insets of Fig. 1 (using TPA as linker[78]) and in Fig. 6c (using as linker a longer analogue of TPA, 4,1′,4′,1″-terphenyl-1,4″-dicarboxylic acid or TDA[81]). Both networks are thermally robust. Because the networks 'compartmentalize' the copper substrate into nanometre-sized cavities, they can steer the

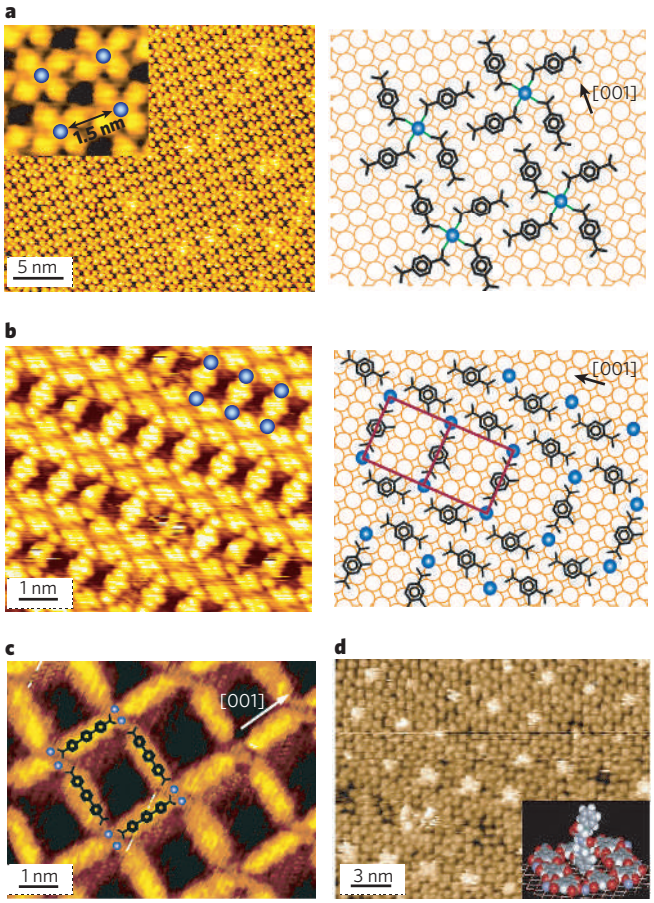

Figure 6 | Metallosupramolecular assembly of low-dimensional Fe-carboxylate coordination systems on a square Cu(100) substrate. **a**, The mononuclear $Fe(TPA)_4$ complexes are stabilized by metal–ligand interactions. Their perfect ordering in a (6×6) square array with periodicity 15 Å is mediated by substrate templating and weak intercomplex hydrogen bridges[78]. **b**, One-dimensional Fe-trimellate coordination polymer with a higher coverage ratio of Fe per tecton. In the ladder structure indicated, with a (4×4) repeat unit, there is a continuous 1D Fe-carboxylate linkage framing open cavities[80]. **c**, Using a linear terphenyl dicarboxylate species as linker with increased length, regular 2D reticulated coordination networks with nanometre-sized cavities are obtained[81]. **d**, Site-selective uptake of L, L-diphenylalanine peptide molecules in a 2D nanoporous Fe-carboxylate architecture[84]; a model for the dipeptide guests in an upright position is depicted in the inset (S. Stepanow, N. Lin, J.V.B. and K.K., unpublished observations).

organization of subsequently deposited molecules, as has been illustrated with C_{60} molecules[81].

As might be expected, substrate and linker symmetry play an important role in 2D supramolecular engineering of metal–organic surface structures. By replacing the Cu(100) surface with its square symmetry by the anisotropic Cu(110) surface, the 1D anisotropy of the substrate can effectively be transferred to the resulting coordination compounds. Trimesic acid with Cu and Fe on the (110) surface is found to form strictly linear metal–organic coordination chains[82]. The local linker geometry is of equal importance. For instance, whereas TMA linkers with three-fold molecular symmetry can form mononuclear $Fe(TMA)_4$ complexes that resemble their terephthalate $Fe(TPA)_4$ counterparts[83], the complexes cannot assemble into perfectly square arrays but form instead an extended coordination network with a regular arrangement of nanocavities[84]. These nanocavities provide well-defined reaction spaces and can even be used as selective receptors for biomolecules. This is as demonstrated in Fig. 6d where the L, L-diphenylalanine peptide species is used as molecular guest in a two-dimensional metal-carboxylate host-system (S. Stepanow, N. Lin, J.V.B. and K.K.,

unpublished observation). The design principles established for 3D carboxylate framework reticular synthesis[85,86] can thus also guide the design of 2D supramolecular metal–organic systems. That is, careful selection of suitable linker structures (in conjunction with appropriate metals) provides an effective strategy for adjusting the size of the cavities or pores present in the 2D assemblies, and the chemical functionalities lining the 'walls' of the pores are determined by the characteristics of the side groups present in the linker. Given the immense wealth and scope of reticular chemistry, a wide range of surface-supported structures with pores of different sizes and chemical characteristics should in principle be accessible. These might find use in the fabrication of patterned surface templates, for the control of host–guest chemistry involving surface structures, or in heterogeneous catalysis in which reactants can interact with the substrate and the supramolecular metal–organic surface structures.

Outlook

Self-organized growth and self-assembly at surfaces can serve as an efficient and versatile tool for creating low-dimensional nanostructures. It offers exquisite control over feature size and organization on the atomic and mesoscopic length scales. We believe that these process characteristics, in combination with the ability to produce high-density structures in a fast and parallel fashion, are essential requirements for any nanofabrication methodology that aims to contribute to the quest for further miniaturization in the microelectronics industry and elsewhere. However, even though processes that make use of self-ordering growth have already yielded systems with intriguing functional properties, many challenges still need to be addressed before such strategies find wide practical use. For example, the incorporation of nanostructures into more complex organized architectures and their effective interfacing to the macroscopic world are vital for any applications. We would expect that this can be achieved by combining bottom-up and top-down techniques, with the former providing ready access to features with sizes below 10 nm, and the latter allowing for integration of these structures into larger functional systems. This general approach should also result in new materials and devices that might find use beyond the applications traditionally targeted by miniaturization efforts, particularly when it is guided by new insights into the physics of small systems or combined with chemical[35,41,87,88] and biological[89–91] bottom-up methods. ■

1. Feynman, R. P. There's plenty of room at the bottom. *Eng. Sci.* **23,** 22–36 (1960).
2. Binnig, G. & Rohrer, H. Scanning tunneling microscopy — from birth to adolescence. *Rev. Mod. Phys.* **59,** 615–625 (1987).
3. Eigler, D. M. & Schweizer, E. K. Positioning single atoms with a scanning tunnelling microscope. *Nature* **344,** 524–526 (1990).
4. Kastner, M. A. Artificial atoms. *Phys. Today* **46,** 24–31 (1993).
5. Dekker, C. Carbon nanotubes as molecular quantum wires. *Phys. Today* **52,** 22–28 (1999).
6. Bohr, M. T. Nanotechnology goals and challenges for electronics applications. *IEEE Trans. Nanotechnol.* **1,** 56–62 (2002).
7. Thomson, D. A. & Best, J. S. The future of magnetic data storage technology. *IBM J. Res. Dev.* **3,** 311–321 (2000).
8. Gates, B. D. *et al*. New approaches to nanofabrication: molding, printing, and other techniques. *Chem. Rev.* **105,** 1171–1196 (2005).
9. Ito, T. & Okazaki, S. Pushing the limits of lithography. *Nature* **406,** 1027–1031 (2000).
10. Xia, Y. N., Rogers, J. A., Paul, K. E. & Whitesides, G. M. Unconventional methods for fabricating and patterning nanostructures. *Chem. Rev.* **99,** 1823–1848 (1999).
11. Vettiger, P. *et al*. The 'millipede'-nanotechnology entering data storage. *IEEE Trans. Nanotechnol.* **1,** 39–55 (2002).
12. Lindsey, J. S. Self-assembly in synthetic routes to devices. Biological principles and chemical perspectives: a review. *New J. Chem.* **15,** 153–180 (1991).
13. Whitesides, G. M., Mathias, J. P. & Seto, C. T. Molecular self-assembly and nanochemistry — a chemical strategy for the synthesis of nanostructures. *Science* **254,** 1312–1319 (1991).
14. Philp, D. & Stoddart, J. F. Self-assembly in natural and unnatural systems. *Angew. Chem. Int. Edn Engl.* **35,** 1154–1196 (1996).
15. Nicolis, G. & Prigogine, I. *Self-Organization in Non-Equilibrium Systems: From Dissipative Structure Formation to Order through Fluctuations* (Wiley, New York, 1977).
16. Eigen, M. Self-organization of matter and the evolution of biological macromolecules. *Naturwissenschaften* **33,** 465–523 (1971).
17. Zhang, Z. Y. & Lagally, M. G. Atomistic processes in the early stages of thin-film growth. *Science* **276,** 377–383 (1997).
18. Brune, H. Microscopic view of epitaxial growth: nucleation and aggregation. *Surf. Sci. Rep.* **31,** 121–229 (1998).
19. Barth, J. V. Transport of adsorbates at metal surfaces : From thermal migration to hot precursors. *Surf. Sci. Rep.* **40,** 75–150 (2000).
20. Röder, H., Hahn, E., Brune, H., Bucher, J. P. & Kern, K. Building one-dimensional and two-dimensional nanostructures by diffusion-controlled aggregation at surfaces. *Nature* **366,** 141–143 (1993).
21. Brune, H., Giovannini, M., Bromann, K. & Kern, K. Self-organized growth of nanostructure arrays on strain-relief patterns. *Nature* **394,** 451–453 (1998).
22. Li, J. L. *et al*. Spontaneous assembly of perfectly ordered identical-size nanocluster arrays. *Phys. Rev. Lett.* **88,** 066101 (2002).
23. Lehn, J.-M. *Supramolecular Chemistry, Concepts and Perspectives* (VCH, Weinheim, 1995).
24. Gimzewski, J. K. & Joachim, C. Nanoscale science of single molecules using local probes. *Science* **283,** 1683–1688 (1999).
25. Rosei, F. *et al*. Properties of large organic molecules at surfaces. *Prog. Surf. Sci.* **71,** 95–146 (2003).
26. Barth, J. V. *et al*. Building supramolecular nanostructures at surfaces by hydrogen bonding. *Angew. Chem. Int. Edn Engl.* **39,** 1230–1234 (2000).
27. Ibach, H. The role of surface stress in reconstruction, epitaxial growth and stabilization of mesoscopic structures. *Surf. Sci. Rep.* **29,** 193–263 (1997).
28. Barth, J. V., Brune, H., Ertl, G. & Behm, R. J. Scanning tunneling microscopy observations on the reconstructed Au(111) surface — atomic structure, long-range superstructure, rotational domains, and surface defects. *Phys. Rev. B* **42,** 9307–9318 (1990).
29. Kern, K. *et al*. Long-range spatial self-organization in the adsorbate-induced restructuring of surfaces — Cu(110)-(2x1)O. *Phys. Rev. Lett.* **67,** 855–858 (1991).
30. Teichert, C. Self-organization of nanostructures in semiconductor heteroepitaxy. *Phys. Rep.* **365,** 335–432 (2002).
31. Bruno, P. Tight-binding approach to the orbital magnetic moment and magnetocrystalline anisotropy of transition-metal monolayers. *Phys. Rev. B* **39,** 865–868 (1989).
32. van der Laan, G. Microscopic origin of magnetocrystalline anisotropy in transition metal thin films. *J. Phys. Cond. Mat.* **10,** 3239–3253 (1998).
33. Wildberger, K., Stepanyuk, V. S., Lang, P., Zeller, R. & Dederichs, P. H. Magnetic nanostructures — 4d clusters on Ag(001). *Phys. Rev. Lett.* **75,** 509–512 (1995).
34. Himpsel, F. J., Ortega, J. E., Mankey, G. J. & Willis, R. F. Magnetic nanostructures. *Adv. Phys.* **47,** 511–597 (1998).
35. Sun, S., Murray, C. B., Weller, D., Folks, L. & Moser, A. Monodisperse FePt nanoparticles and ferromagnetic FePt nanocrystal superlattices. *Science* **287,** 1989–1992 (2000).
36. Gambardella, P., Blanc, M., Brune, H., Kuhnke, K. & Kern, K. One-dimensional metal chains on Pt vicinal surfaces. *Phys. Rev. B* **61,** 2254–2262 (2000).
37. Kuhnke, K. & Kern, K. Vicinal metal surfaces as nanotemplates for the growth of low-dimensional structures. *J. Phys. Cond. Mat.* **15,** S3311–S3335 (2003).
38. Rusponi, S. *et al*. The remarkable difference between surface and step atoms in the magnetic anisotropy of two-dimensional nanostructures. *Nature Mater.* **2,** 546–551 (2003).
39. Gambardella, P. *et al*. Ferromagnetism in one-dimensional monatomic metal chains. *Nature* **416,** 301–304 (2002).
40. Gambardella, P. *et al*. Giant magnetic anisotropy of single cobalt atoms and nanoparticles. *Science* **300,** 1130–1133 (2003).
41. Gambardella, P. *et al*. Oscillatory magnetic anisotropy in one-dimensional atomic wires. *Phys. Rev. Lett.* **93,** 077203 (2004).
42. Bimberg, D., Grundmann, M. & Ledentsov, N. N. *Quantum Dot Heterostructures* (Wiley, Chichester, 1999).
43. Costantini, G. *et al*. Universal island shapes of self-organized semiconductor quantum dots. *Appl. Phys. Lett.* **85,** 5673–5675 (2004).
44. Daruka, I., Tersoff, J. & Barabasi, A. L. Shape transition in growth of strained islands. *Phys. Rev. Lett.* **82,** 2753–2756 (1999).
45. Warburton, R. J. *et al*. Optical emission from a charge-tunable quantum ring. *Nature* **405,** 926–929 (2000).
46. Michler, P. *et al*. A quantum dot single-photon turnstile device. *Science* **290,** 2282–2284 (2000).
47. Burkard, G., Loss, D. & DiVincenzo, D. P. Coupled quantum dots as quantum gates. *Phys. Rev. B* **59,** 2070–2078 (1999).
48. Cole, T. & Lusth, J. C. Quantum-dot cellular automata. *Prog. Quantum Electron.* **25,** 165–189 (2001).
49. Shchukin, V. A. & Bimberg, D. Spontaneous ordering of nanostructures on crystal surfaces. *Rev. Mod. Phys.* **71,** 1125–1171 (1999).
50. Heidemeyer, H., Denker, U., Müller, C. & Schmidt, O. G. Morphology response to strain field interferences in stacks of highly ordered quantum dot arrays. *Phys. Rev. Lett.* **91,** 196103 (2003).
51. Lee, H., Johnson, J. A., He, M. Y., Speck, J. S. & Petroff, P. M. Strain-engineered self-assembled semiconductor quantum dot lattices. *Appl. Phys. Lett.* **78,** 105–107 (2001).
52. Arakawa, Y. & Sakaki, H. Multidimensional quantum well laser and temperature-dependence of its threshold current. *Appl. Phys. Lett.* **40,** 939–941 (1982).
53. Nakajima, F., Miyoshi, Y., Motohisa, J. & Fukui, T. Single-electron AND/NAND logic circuits based on a self-organized dot network. *Appl. Phys. Lett.* **83,** 2680–2682 (2003).
54. Feynman, R. P. Simulating physics with computers. *Int. J. Theor. Phys.* **21,** 467–488 (1982).
55. Shor, P. in *Proc 35th Annu. Symp. Foundations of Computer Science* (IEEE, Los Alamitos, 1994).
56. Deutsch, D. Quantum theory, the Church–Turing principle and the universal quantum computer. *Proc. R. Soc. Lond. A* **400,** 97–117 (1985).
57. Barenco, A. *et al*. Elementary gates for quantum computation. *Phys. Rev. A* **52,** 3457–3467 (1995).
58. Schedelbeck, G., Wegscheider, W., Bichler, M. & Abstreiter, G. Coupled quantum dots fabricated by cleaved edge overgrowth: From artificial atoms to molecules. *Science* **278,** 1792–1795 (1997).
59. Bayer, M. *et al*. Coupling and entangling of quantum states in quantum dot molecules. *Science* **291,** 451–453 (2001).
60. Songmuang, R., Kiravittaya, S. & Schmidt, O. G. Formation of lateral quantum dot molecules around self-assembled nanoholes. *Appl. Phys. Lett.* **82,** 2892–2894 (2003).
61. Deng, X. & Krishnamurthy, M. Self-assembly of quantum-dot molecules: heterogeneous nucleation of SiGe islands on Si(100). *Phys. Rev. Lett.* **81,** 1473–1476 (1998).
62. Prins, L. J., Reinhoudt, D. N. & Timmerman, P. Non-covalent synthesis using hydrogen bonding. *Angew. Chem. Int. Edn Engl.* **40,** 2382 (2001).
63. Barth, J. V., Weckesser, J., Lin, N., Dmitriev, S. & Kern, K. Supramolecular architectures and nanostructures at surfaces. *Appl. Phys. A* **76,** 645 (2003).

64. Feyter, S. D. & Schryver, F. C. D. Two-dimensional supramolecular self-assembly probed by scanning tunneling microscopy. *Chem. Soc. Rev.* **32,** 139–150 (2003).
65. Lin, N., Dmitriev, A., Weckesser, J., Barth, J. V. & Kern, K. Real-time single-molecule imaging of the formation and dynamics of coordination compounds. *Angew. Chem. Int. Edn Engl.* **41,** 4779 (2002).
66. Lukas, S., Witte, G. & Wöll, C. Novel mechanism for molecular self-assembly on metal substrates : unidirectional rows of pentacene on Cu(110) produced by substrate-mediated repulsion. *Phys. Rev. Lett.* **88,** 028301 (2002).
67. Yokoyama, T., Yokoyama, S., Kamikado, T., Okuno, Y. & Mashiko, S. Selective assembly on a surface of supramolecular aggregates of controlled size and shape. *Nature* **413,** 619–621 (2001).
68. Böhringer, M. *et al*. Two-dimensional self-assembly of supramolecular clusters and chains. *Phys. Rev. Lett*. **83**, 324–327 (1999).
69. Otero, R. *et al*. One-dimensional assembly and selective orientation of Lander molecules on an O-Cu template. *Angew. Chem. Int. Edn Engl.* **43,** 2092–2095 (2004).
70. Clair, S., Pons, S., Brune, H., Kern, K. & Barth, J. V. Mesoscopic metallosupramolecular texturing through hierarchic assembly. *Angew. Chem. Int. Edn Engl.* (in the press).
71. Barth, J. V. *et al*. Stereochemical effects in supramolecular self-assembly at surfaces: 1-D vs. 2-D enantiomorphic ordering for PVBA and PEBA on Ag(111). *J. Am. Chem. Soc.* **124,** 7991–8000 (2002).
72. Weckesser, J., Vita, A. D., Barth, J. V., Cai, C. & Kern, K. Mesoscopic correlation of supramolecular chirality in one-dimensional hydrogen-bonded assemblies. *Phys. Rev. Lett.* **87,** 096101 (2001).
73. Dmitriev, A., Lin, N., Weckesser, J., Barth, J. V. & Kern, K. Supramolecular assemblies of trimesic acid on a Cu(100) surface. *J. Phys. Chem. B* **106,** 6907–6912 (2002).
74. Griessl, S., Lackinger, M., Edelwirth, M., Hietschold, M. & Heckl, W. M. Self-assembled two-dimensional molecular host-guest architectures from trimesic acid. *Single Molecules* **3,** 25–31 (2002).
75. Theobald, J. A., Oxtoby, N. S., Phillips, M. A., Champness, N. R. & Beton, P. H. Controlling molecular deposition and layer structure with supramolecular surface assemblies. *Nature* **424,** 1029–1031 (2003).
76. Leininger, S., Olenyuk, B. & Stang, P. J. Self-assembly of discrete cyclic nanostructures mediated by transition metals. *Chem. Rev.* **100,** 853–908 (2000).
77. Holiday, B. J. & Mirkin, C. A. Strategies for the construction of supramolecular compounds through coordination chemistry. *Angew. Chem. Int. Edn Engl.* **40,** 2022–2043 (2002).
78. Lingenfelder, M. *et al*. Towards surface-supported supramolecular architectures: tailored coordination assembly of 1,4-benzenedicarboxylate and Fe on Cu(100). *Chem. Eur. J.* **10,** 1913–1919 (2004).
79. Dmitriev, A. *et al*. Design of extended surface-supported chiral metal-organic arrays comprising mononuclear iron centers. *Langmuir* **41,** 4799–4801 (2004).
80. Dmitriev, A., Spillmann, H., Lin, N., Barth, J. V. & Kern, K. Modular assembly of two-dimensional metal-organic coordination networks at a metal surface. *Angew. Chem. Int. Edn Engl.* **41,** 2670–2673 (2003).
81. Stepanow, S. *et al*. Steering molecular organization and host-guest interactions using tailor-made two-dimensional nanoporous coordination systems. *Nature Mater.* **3,** 229–233 (2004).
82. Classen, T. *et al*. Templated growth of metal-organic coordination chains at surfaces. *Angew. Chem. Int. Edn Engl.* (in the press).
83. Messina, P. *et al*. Direct observation of chiral metal-organic complexes assembled on a Cu(100) surface. *J. Am. Chem. Soc.* **124,** 14000–14001 (2002).
84. Spillmann, H. *et al*. Hierarchical assembly of two-dimensional homochiral nanocavity arrays. *J. Am. Chem. Soc.* **125,** 10725–10728 (2003).
85. Yaghi, O. M. *et al*. Reticular synthesis and the design of new materials. *Nature* **423,** 705–714 (2003).
86. Kitagawa, S., Kitaura, R. & Noro, S. Functional coordination polymers. *Angew. Chem. Int. Edn Engl.* **43,** 2334–2375 (2004).
87. Joachim, C., Gimzewski, J. K. & Aviram, A. Electronics using hybrid-molecular and mono-molecular devices. *Nature* **408,** 541–548 (2000).
88. Ouyang, M. & Awscholom, D. D. Coherent spin transfer between molecularly bridged quantum dots. *Science* **301,** 1074–1078 (2003).
89. Niemeyer, C. M. Nanoparticles, proteins and nucleic acids: biotechnology meets materials science. *Angew. Chem. Int. Edn Engl.* **40,** 4128–4158 (2001).
90. Seeman, N. C. & Belcher, A. M. Emulating biology: Building nanostructures from the bottom up. *Proc. Natl Acad. Sci. USA* **99,** 6451–6455 (2002).
91. Sarikaya, M., Tamerler, C., Jen, A. K. Y., Schulten, K. & Baneyx, F. Molecular biomimetics: nanotechnology through biology. *Nature Mater.* **2,** 577–585 (2003).
92. Cleland, A. N. & Roukes, M. L. A nanometre-scale mechanical electrometer. *Nature* **392,** 160–162 (1998).
93. Kind, H. *et al*. Patterned films of nanotubes using microcontact printing of catalysts. *Adv. Mater.* **11,** 1285–1289 (1999).
94. Tans, S. J., Devoret, M. H., Groeneveld, R. J. A. & Dekker, C. Electron–electron correlations in carbon nanotubes. *Nature* **394,** 761–764 (1998).
95. Ross, F. M., Tromp, R. M. & Reuter, M. C. Transition states between pyramids and domes during Ge/Si island growth. *Science* **286,** 1931–1934 (1999).
96. Corso, M. *et al*. Boron nitride nanomesh. *Science* **303,** 217–220 (2004).

Acknowledgements K.K. thanks the many students, postdocs and scientific collaborators who have contributed to the exploration of the atomic world of surfaces and nanostructures. Special thanks go to N. Lin for his enthusiasm in advancing the concepts of supramolecular chemistry at surfaces.

Author Information Reprints and permissions information is available at npg.nature.com/reprintsandpermissions. The authors declare no competing financial interests. Correspondence and requests for materials should be addressed to K.K. (k.kern@fkf.mpg.de).